Volume 29 Number 14 30 July 2009 ISSN 0278-4343

ELSEVIER

CONTINENTAL SHELF RESEARCH

Research Papers

Continued on outside back cover

www.elsevier.com/locate/csr

Continental Shelf Research 29 (2009) 1697–1710

Contents lists available at ScienceDirect

Continental Shelf Research

journal homepage: www.elsevier.com/locate/csr

Seasonal changes in larval fish assemblages in a semi-enclosed sea (Gulf of California)

L. Sánchez-Velasco [a,*], M.F. Lavín [b,1], M. Peguero-Icaza [c], C.A. León-Chávez [a], F. Contreras-Catala [a], S.G. Marinone [b,1], I.V. Gutiérrez-Palacios [d], V.M. Godínez [b,1]

[a] Centro Interdisciplinario de Ciencias Marinas, Ave. Inst. Politécnico Nacional s/n, La Paz BCS, 2300, México
[b] Centro de Investigación Científica y de Educación Superior de Ensenada, Km 107, Carretera Tijuana-Ensenada, Ensenada, BC, 22860, México
[c] Centro de Investigación Científica y de Educación Superior de Ensenada, Estación La Paz Miraflores 334, Col. Bella Vista, La Paz. BCS, 23050, México
[d] Estación de Investigación Oceanográfica de Ensenada, Secretaría de Marina. Boulevard Costero Esquina Sangines S/N. Ensenada, BC, 22800, México

ARTICLE INFO

Article history:
Received 8 January 2009
Received in revised form
25 May 2009
Accepted 2 June 2009
Available online 18 June 2009

Keywords:
Larval fish assemblages
Mesoscale hydrographic structures
Circulation
Mexico
Gulf of California

ABSTRACT

The northern Gulf of California (NGC) is characterized by seasonal hydrography and circulation (cyclonic in summer and anticyclonic in winter), by intense tidal mixing in the midriff archipelago region (MAR), and by coastal upwelling on the eastern side from autumn to spring. We examined changes in larval fish assemblages (LFAs) in relation with hydrography and circulation during both phases of the seasonal circulation, as indicators of changes in the pelagic ecosystem. A canonical correspondence analysis defined LFAs ($r>0.70$), which were related with: (i) the coastal current on the mainland shelf, (ii) the central eddy and (iii) the MAR. In the early cyclonic phase, when the temperature and stratification were increasing and the coastal current was starting, demersal (*Gobulus crescentalis, Lythrypnus dalli*) and mesopelagic species (*Benthosema panamense*) dominated the NGC. The highest larval abundance was in the Current LFA area and the lowest in the MAR LFA area. In the mature cyclonic phase, the larval abundance increased in the NGC and species characteristic of eastern boundary current systems such as *Opisthonema libertate* and *Engraulis mordax* displaced the demersal species and became dominant, together with *B. panamense* in the Current LFA area; the latter species dominated in the Eddy LFA area. In the early anticyclonic phase, the direction of the coastal current reversed and the temperature and larval abundance decreased. *E. mordax* and *B. panamense* larvae continued dominating the NGC with higher abundance in the MAR than in the Current and Eddy LFA areas. In the mature anticyclonic phase, *E. mordax* larvae dominated in the Current and the Eddy LFA areas with the highest abundance in the former, while *M. productus* larvae (an eastern boundary current species) dominated in the Eddy LFA area. Results showed that in the NGC, the dramatically seasonal and predictable hydrographic and circulation features trigger the seasonal spawning of the dominant species. The biological richness of the coastal current area, in both circulation phases, suggested that this area has an important role in the pelagic ecosystem functionality of the NGC.

1. Introduction

It is known that the temporal coupling between fish species spawning and mesoscale hydrographic structures such as eddies, meanders and fronts increases larval survival (Iles and Sinclair, 1982). These structures act as mechanisms for enrichment, concentration and retention of plankton organisms (fish larvae and their prey) (Bakun, 1996), and can contribute to the formation of larval fish assemblages (LFAs) with hydrographically well-defined boundaries (e.g., Moser and Smith, 1993; Peguero-Icaza et al., 2008). However, the evolution of the relationships between LFAs and hydrography at the seasonal time scale is less well known.

The Gulf of California (GC, insert, Fig. 1a), a subtropical semi-enclosed sea, is very seasonal, not only in the near-surface thermohaline properties and water-column structure but also in its circulation, which is cyclonic in summer and anticyclonic in winter (see review by Lavín and Marinone, 2003). Although mesoscale structures such as fronts, meanders and eddies are common in the Gulf (Pegau et al., 2002; Navarro-Olache et al., 2004; Lopez-Calderon et al., 2008), the seasonal component of the circulation is remarkably predictable, and, in the northern Gulf of California (NGC, Fig. 1a), dominant in time scales longer than a week (Peguero-Icaza et al., 2008; Marinone et al., 2008). Theoretical and numerical studies indicate that the seasonal

* Corresponding author. Tel.: +52 612 12 2 61 85; fax: +52 612 12 2 53 22.
E-mail addresses: lsvelasc@gmail.com, lsvelasc@ipn.mx (L. Sánchez-Velasco).
[1] Tel.: +52 646 17 5 05 00; fax: +52 646 1 75 05 47.

0278-4343/$ - see front matter © 2009 Elsevier Ltd. All rights reserved.
doi:10.1016/j.csr.2009.06.001

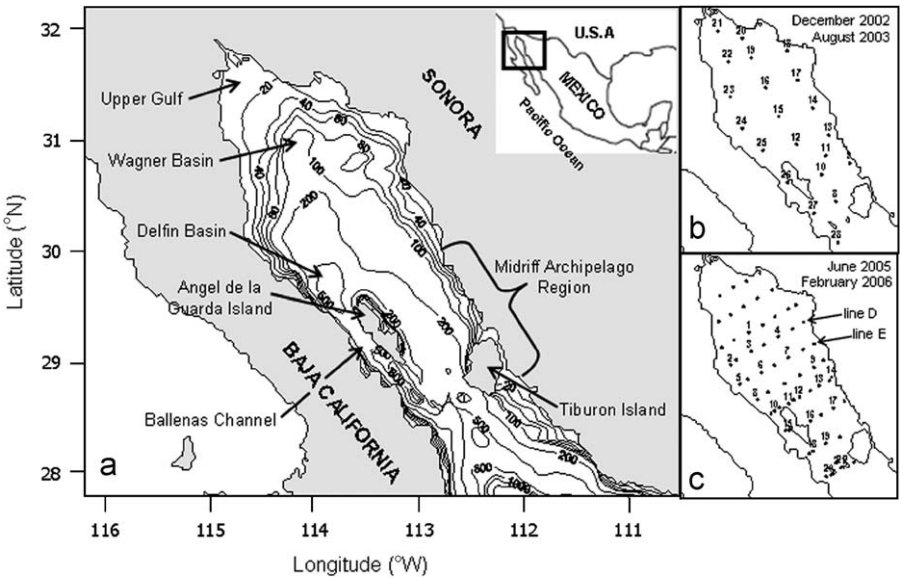

Fig. 1. (a) Bathymetry of the northern Gulf of California (depth in meters), with named places and basins. (b) and (c) Show the sampling grids of each cruise. In (c) the position of Lines D and E are shown for later reference.

circulation of the GC is caused by internal Kelvin-like waves of annual period driven by the Pacific Ocean and by the seasonal wind (Beier, 1997; Ripa, 1997).

Two inter-related aspects of the seasonally reversing circulation in the NGC are an eddy in the center of the basin, and a coastal current on the mainland shelf. Direct observations show that the central eddy is ~150 m deep, cyclonic from June to September and anticyclonic from November to April (Palacios-Hernández et al., 2002; Carrillo et al., 2002). The coastal current flows poleward during the cyclonic period (summer) and equatorward during the anticyclonic period (winter). Numerical models (Marinone, 2003; Zamudio et al., 2008) and recent direct observations (Lavín et al., 2009) suggest that in summer this coastal current is present as far as the GC entrance.

While the southern GC is very deep (1500–3000 m) and tidal currents there are weak, most of the NGC is less than 200 m deep and tidal mixing is very important (Paden et al., 1991; Argote et al., 1995), especially around the sills of the midriff archipelago region (MAR) (Fig. 1a) and in the shallow Upper Gulf (<30 m deep). Ballenas Channel is a deep (800–1600 m) sub-province of the NGC where tidal mixing and convergence-induced upwelling generate hydrographic conditions that are very different from those in the rest of the GC: stratification tends to be weaker, deep water is warm (~11 °C), while its sea-surface temperature (SST) is the lowest in the Gulf (Paden et al., 1991; Argote et al., 1995; López et al., 2006). The MAR, especially Ballenas Channel and the sills, is an area of continuous upward pumping of nutrients by tidal mixing and convergence-induced upwelling (Alvarez-Borrego and Lara-Lara, 1991; López et al., 2006), while in the Upper Gulf tidal mixing has the same effect. This combines with the residual circulation to make the entire NGC a very productive area (Santamaría-del-Angel et al., 1994a; Hidalgo-González and Alvarez-Borrego, 2004).

The GC supports a high-diversity, high-abundance fish fauna of commercial and ecological importance (e.g., Moser et al., 1974). Most of the fish species have well-defined spawning periods: species such as the epipelagic *Sardinops sagax* and *Engraulis mordax*, and the deep demersal *Merluccius productus* spawn from November to April, with maximum intensity in January and February (e.g., Hammann et al., 1998; Green-Ruíz and Hinojosa-Corona, 1997), while the epipelagic *Auxis* spp. and *Opisthonema libertate* and the mesopelagic *Benthosema panamense* spawn mainly from June to September with a spawning peak in August (e.g., Avalos-García et al., 2003; Aceves-Medina et al., 2004). However, the relationships of these spawning periods with the oceanographic processes that occur in the GC at those times have not been made clear.

Although there are studies on the GC that relate LFAs with SST (e.g., Avalos-García et al., 2003; Sánchez-Velasco et al., 2004; Aceves-Medina et al., 2004) and with circulation (e.g., Sánchez-Velasco et al., 2006; Peguero-Icaza et al., 2008), the seasonal evolution of the coupling between the distribution of LFAs and oceanographic processes has not been addressed in an integral way. Considering the presence of areas of continuous enrichment and the predictability of the seasonal circulation of the NGC, it may be possible to identify the physical processes whose changes trigger the seasonal spawning (and control the distribution of the larvae) of the dominant species of the different adult habits, such as coastal pelagic (e.g., *S. sagax, E. mordax, O. libertate*), demersal deep (e.g., *M. productus*) and mesopelagic (e.g., *B. panamense, Triphoturus mexicanus*). This is especially interesting given the presence in the NGC of markedly different environments in a relatively confined area. Therefore, the study of this physical–biological coupling at the seasonal time scale will provide knowledge of the functionality of the pelagic ecosystem in general.

The aim of this study is to examine the seasonal changes in LFAs and their boundaries, and to relate them with the seasonal changes of the hydrography and the circulation in the NGC. We used data collected during periods representative of the cyclonic (June and August) and anticyclonic (December and February) phases of the seasonal circulation.

2. Methods

Plankton and physical data were collected during four oceanographic cruises (Table 1), two representing the anticyclonic phase (December 2002 and February 2006), and two representing the cyclonic phase (August 2003 and June 2005) of the seasonal circulation. The CTD sampling stations are shown as dots in Fig. 1b and c and those for biological samples (~23 stations in each cruise) are marked with numbers.

Vertical profiles of temperature and salinity were obtained at each station with a factory-calibrated Sea-Bird Electronics

Table 1
General information of cruises made in the northern Gulf of California and the circulation phases according to Palacios-Hernández et al. (2002).

Cruise dates:	December 7–13, 2002	August 1–6, 2003	June 2–11, 2005	February 9–23, 2006
Phase of seasonal circulation	Anticyclonic	Mature cyclonic	Early cyclonic	Mature anticyclonic
Research vessel	*R/V Francisco de Ulloa*[1]	*R/V Francisco de Ulloa*	*R/V Altair*[2]	*R/V Altair*

(1) CICESE, (2) Secretaría de Marina, México.

Conductivity Temperature Depth (CTD) Profiler model SB-19, with dissolved oxygen (O_2) sensor. Geostrophic currents in vertical sections were calculated relative to minimum common sampling depth between pairs of stations, after subjecting the temperature and salinity data to objective analysis to eliminate internal waves and other high frequency noise. In addition to the field data, mean weekly images of chlorophyll and SST were obtained from the AQUA-MODIS satellites (4 km × 4 km resolution) as support for the interpretation of the hydrographic data, in particular to identify features such as eddies and fronts (www.oceancolor.gsfc.nasa.gov/cgi/level3).

To provide a description of the expected circulation in the GC at the time of the cruises, the outputs of the three-dimensional baroclinic numerical model of Marinone (2003) were used. This model gives an acceptable description of the mean and seasonal overall circulation, and has previously been used to describe the fate of particles released in the GC, as an approximation to larval transport (Marinone et al., 2008; Cudney-Bueno et al., 2009). The model domain has a mesh size of 2.5′ × 2.5′ (~3.9 km × 4.6 km) in the horizontal and 12 layers in the vertical. It is forced with the climatological annual variability of hydrography at the mouth, sinusoidal up-down-gulf wind of annual period and tides.

Zooplankton hauls were made using a Bongo net with a mouth diameter of 60 cm and mesh size of 505 and 333 μm. Hauls were oblique from near the bottom to the surface or from 200 m depth to the surface when bottom depth permitted. These hauls were in a circular trajectory at a speed of 2.5 knots, following the methodology recommended by Smith and Richardson (1979). The volume of water filtered was calculated using calibrated flowmeters placed in the mouth of the nets. Each sample was fixed with 5% formalin buffered with sodium borate. Zooplankton biomass (ZB) was estimated by displacement volume (Kramer et al., 1972) and standardized to mL 1000 m^{-3}. Fish larvae were removed from the samples of 505 μm mesh and identified according to descriptions of Moser (1996). Larval abundance was standardized to number of larvae per 10 m^2 of sea surface, following Smith and Richardson (1979).

A canonical correspondence analysis (CCA) (Ter Braak, 1986) was applied to define LFAs in accordance to their location and to environmental indicators in each cruise. Before calculating the CCA, the standardized biological data and the matrix of environmental indicators were root–root transformed, to reduce the weight of the most abundant species (Field et al., 1982). The matrix of environmental parameters contained the average values of temperature, salinity and dissolved oxygen in the top 10 m of the water column, the zooplankton sampling depth and the zooplankton biomass values. The results are shown as biplots (the two first ordination axes) with environmental parameters as a vector and the eligible elements (sampling stations) as points in the ordination space (Ter Braak, 1986; De la Cruz-Agüero, 1994).

The Olmstead–Tukey test was used for hierarchies of the species in each LFA (dominant, frequent, constant and rare species) (e.g., Sánchez-Velasco et al., 2004, 2006). This test considered the average relative abundance against the percentage of the appearance frequency of each species (Sokal and Rohlf, 1985). This is a robust test with a clear interpretation and has been used successfully in the ecological characterization of fish larvae communities (e.g., Sánchez-Velasco et al., 2006; Peguero-Icaza et al., 2008).

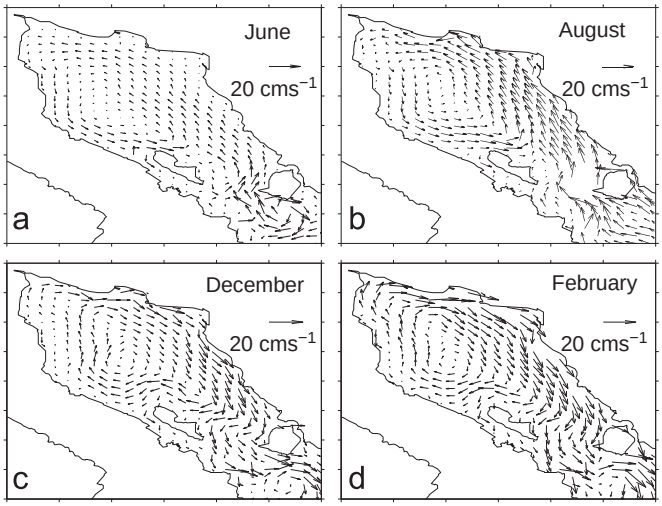

Fig. 2. Monthly mean surface currents (0–10 m) in the northern Gulf of California from the 3D numerical model of Marinone (2003): (a) June 2005, (b) August 2003, (c) December 2002 and (d) February 2006.

3. Results

Results are presented in a seasonal sequence, starting with the cyclonic phase (June and August cruises) and following with the anticyclonic phase (December and February cruises) (Table 1).

3.1. Circulation and hydrography

According to the observations-based description of the seasonal circulation (Palacios-Hernández et al., 2002; Carrillo et al., 2002), the June (December) cruise was made in the early stages of the cyclonic (anticyclonic) phase and the August (February) cruise in the mature stage. The monthly averaged surface circulation predicted by the numerical model (Marinone, 2003), shown in Fig. 2, agrees with this overall description.

The vertical contours of temperature across the NGC along Line E (see position in Fig. 1c) during June, shown in Fig. 3a, presented a strong and uplifted thermocline in the center of the basin, suggesting the presence of cyclonic circulation (density is dominated by temperature in the GC; see *T*–*S* diagrams below). This is confirmed by the geostrophic current calculations (Fig. 3b); the poleward coastal current on the mainland side of the NGC was wider and faster (>0.1 ms^{-1}) than the equatorward flow on the peninsula side. The weak currents support the idea that the June cruise was made in the early stages of the cyclonic period, and were in agreement with the model predictions for June (Fig. 2a), although the model speeds were weaker. The model predictions for August (Fig. 2b) showed that the circulation pattern was similar to that in June but ~50% stronger. There were too few CTD stations to draw vertical contours of temperature and geostrophic

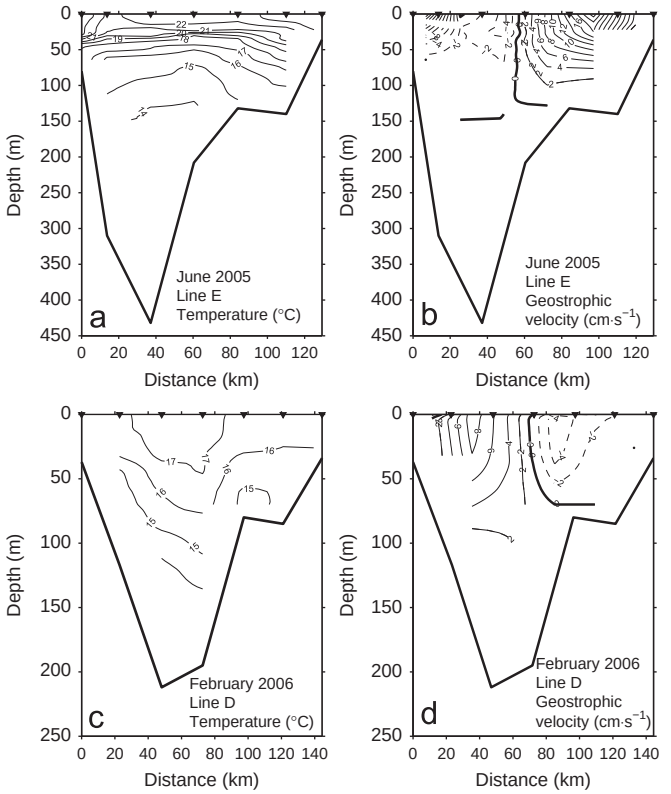

Fig. 3. Vertical distribution of temperature (°C) and geostrophic velocity (cm s^{-1}), relative to minimum common sampling depth of pairs of stations, across the northern Gulf of California. (a) Temperature, June 2005, Line E; (b) Geostrophic velocity, June 2005, Line E; (c) Temperature, February 2006, Line D; (d) Geostrophic velocity, February 2006, Line D. See Line positions in Figs. 1c, 5a,b and 6c,d. Black triangles indicate CTD stations.

velocity for August, but the cyclonic circulation for August was supported by the geopotential anomaly relative to 50 m (not shown), which presented a low in the center of the NGC.

For December (Fig. 2c), the model predicted that anticyclonic circulation covered the entire NGC. The fastest currents were again found on the mainland shelf (<0.10 m s^{-1}), but now the coastal current on the mainland shelf flowed to the southeast to form an overall flow out of the NGC. The vertical contours of temperature across the NGC along Line D (see position in Fig. 1c) during February, shown in Fig. 3c, presented weak stratification (surface mixed layer ~70 m) and depressed isotherms in the center of the basin, suggesting anticyclonic circulation. The geostrophic current calculations (Fig. 3d) produced weak equatorward speeds (<0.05 ms^{-1}) on the mainland side of the NGC and a better defined poleward flow on the peninsula side. The weak geostrophic currents found here are similar to those reported from the anticyclonic period by Carrillo et al., (2002) and Palacios-Hernández et al. (2002). In winter, the circulation in the NGC is a mixture of barotropic and baroclinic, therefore the geostrophic calculations produced weaker currents than direct observations and numerical models. The model predictions for February (Fig. 2d) show a circulation similar to that in December but more intense in general especially close to shore on the mainland side.

The seasonal evolution of the vertical structure of the hydrography is shown in Fig. 4, using selected temperature profiles and *T*–*S* diagrams from three provinces of the NGC: (A) the eddy area in the center of the NGC, (B) the mainland shelf area and (C) the MAR. Only the top 200 m of the water-column temperature is shown, but the *T*–*S* diagrams include the entire sampled profile. (A) In the central eddy (Fig. 4a), the SST changed from ~22.5 to ~30 °C between June (black line) and August (blue line) while stratification increased sharply. While in summer the surface mixed layer was only a few meters deep by December (orange line) it deepened to ~50 m and cooled to ~21 °C and by February (green line) to ~80 m and ~17 °C, respectively. The *T*–*S* diagram (Fig. 4b) shows that only Gulf of California Water (characterized by $S \geq 34.9$; Lavín et al., 2009) was present, and that the highest (lowest) surface salinity was found in August (February). (B) On the mainland shelf, temperature and stratification increased in the entire water column between June and August (Fig. 4c), and then decreased steadily in December and February. The *T*–*S* diagrams are very similar to those in the central eddy, and both sets showed salinity intrusions in the thermocline during summer. (C) The MAR temperature profiles (Fig. 4e) show that stratification was significant only in August, with maximum SST ~27 °C, some 3 °C cooler than in the other two provinces. In February, the upper 200 m were thoroughly mixed. The *T*–*S* diagrams exhibit the weaker seasonality compared with the other provinces, and show the presence of Subtropical Subsurface Water ($S < 34.9$) in the deeper layers.

The seasonal evolution of the surface (top 10 m average) temperature, salinity and dissolved oxygen distribution, which will be used in the canonical correspondence analysis, is shown in Figs. 5 and 6. For the cruises of the cyclonic phase (June and August, Fig. 5), the distribution pattern of the three variables was similar. In June (Fig. 5a–c), the highest temperature values (23 °C) were in both coasts and to the north of the study area, and the lowest values (18 °C) to the south of the Angel de La Guarda Island. The maximum salinity (35.6) and dissolved oxygen (4.8 mL/L) were found north of the MAR and the minimum values (35.2; 3.0 mL/L) in the south of this zone. In August (Fig. 5d–f), although with the same tendency as in June, the ranges of temperature and salinity increased. The highest values of temperature (31 °C) and salinity (36.0), and the lowest of dissolved oxygen (3.0 mL/L) were found in the Upper Gulf. The lowest temperature (26.5 °C) and salinity (35.4), and highest dissolved oxygen (3.3 mL/L) were in the MAR, where the strongest gradients of temperature and dissolved oxygen were detected. The salinity distribution in August seems to reflect the cyclonic circulation.

In December (Fig. 6a–c), the salinity showed a pattern similar to that in August, but the temperature and the dissolved oxygen changed: the salinity and the dissolved oxygen showed their maxima in the Upper Gulf (36; 3.6 mL/L) and the minima in the MAR (35.4; 3.0 mL/L). The highest temperature (21 °C) was north of the MAR and the lowest (19 °C) in the Upper Gulf. In February, the mature cyclonic phase, the distributions of temperature and salinity suggested the central eddy. The three variables increased their values from the MAR to the NGC, and tended to decrease in the Upper Gulf (Fig. 6d–f). The lowest temperature (14.5 °C), salinity (35) and dissolved oxygen (3.8 mL/L) values were located to the south of the Angel de La Guarda Island and the highest values (17 °C; 35.5; 5.4 mL/L) in the central eddy area.

3.2. Satellite images

The synoptic vision of the MODIS satellite images of SST and chlorophyll (Figs. 7 and 8) showed marked seasonality with the highest values of SST and the lowest values of chlorophyll in August and the lowest values of SST and the highest of chlorophyll in February. In most cases, mesoscale hydrographic structures were observed, the most outstanding being the eddy in the center of the NGC and the SST and chlorophyll fronts in the MAR. The SST patterns shown by the images are similar to those observed directly (Figs. 5a, d and 6a, d) although the observed temperature was lower than in the images.

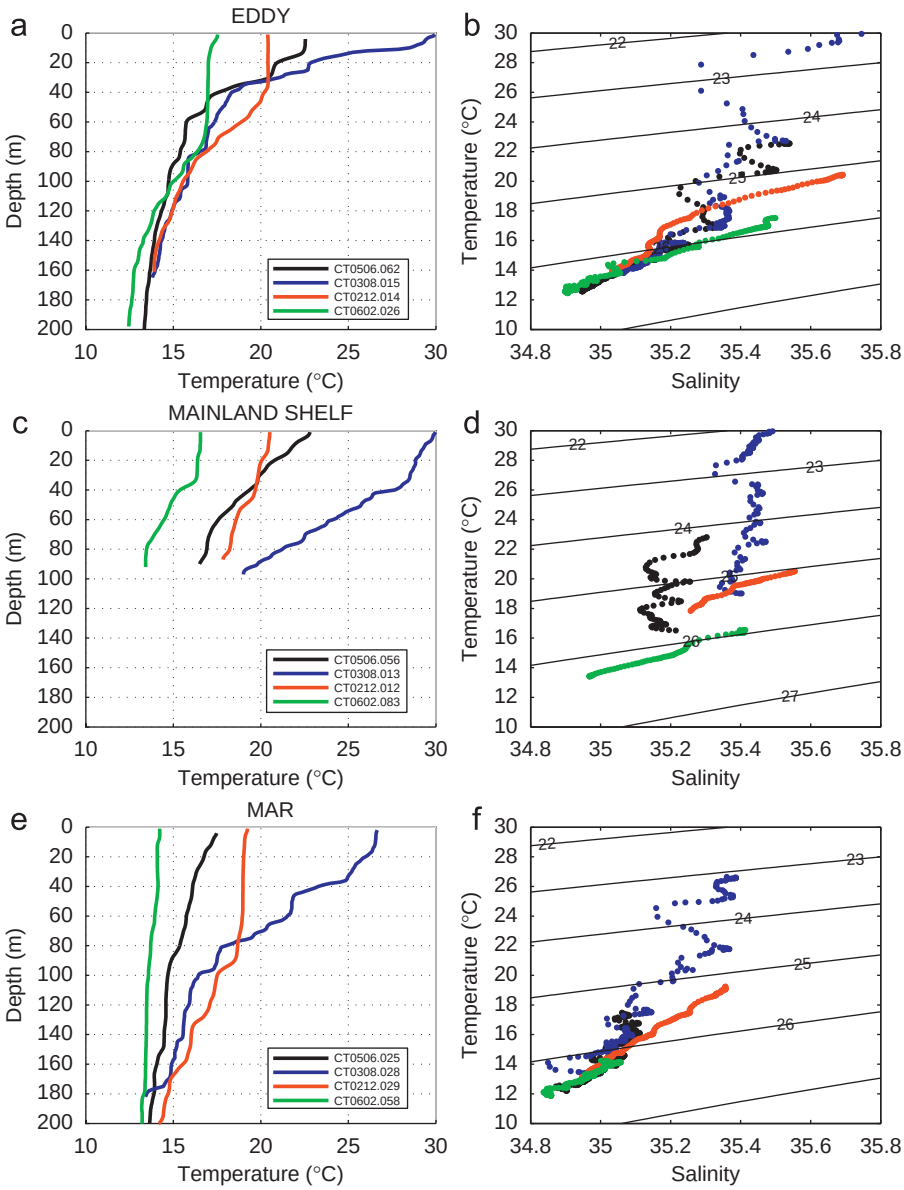

Fig. 4. Seasonal evolution of the vertical hydrographic structure in some provinces of the northern Gulf of California. (a) and (b) Temperature profile and *T*–*S* diagrams from the central eddy area, (c) and (d) Temperature profile and *T*–*S* diagrams from the mainland shelf area. (e) and (f) Temperature profile and *T*–*S* diagrams from the midriff archipelago region (MAR).

In June (Fig. 7a and b), the eddy was not very clear in the images, possibly because (this being the early cyclonic phase) it was still weak, as shown in the temperature and velocity cross-sections of Line E (Fig. 3a and b). The chlorophyll and SST fronts south of the Angel de La Guarda Island, on the other hand, were evident. In August (Fig. 7c and d), the cyclonic eddy was apparent in the chlorophyll image. The eddy area had lower chlorophyll concentration ($<0.3\,mg\,m^{-3}$) and temperature ($<29.5\,^{\circ}C$) that the surroundings. The strongest gradients of SST and chlorophyll were observed south and east of Angel de La Guarda Island.

In December (Fig. 8a and b), the chlorophyll concentration tended to increase and the SST to decrease in relation to August. Although an eddy was not apparent, the SST image suggests trapping on the western side. Surface gradients in the MAR were observed mainly in the temperature image. In February (Fig. 8c and d), the highest chlorophyll values ($>5.0\,mg\,m^{-3}$) were in the mainland side and in the Upper Gulf. The anticyclonic eddy seen in the temperature and geostrophic currents across Line D (Fig. 3c and d) was suggested by both images with lower chlorophyll values ($<2.0\,mg\,m^{-3}$) and higher SST ($>17\,^{\circ}C$) than in its periphery.

3.3. Zooplankton biomass and fish larvae

3.3.1. Zooplankton biomass

In June (Fig. 9a), the highest values of zooplankton biomass ($>500\,mL\ 1000\,m^{-3}$) were clearly located on the mainland side, while the lowest values were north of the MAR ($<200\,mL\ 1000\,m^{-3}$). In August (Fig. 9b), the ZB showed high values ($>500\,mL\ 1000\,m^{-3}$) in the Upper Gulf and on the mainland coastal area, intermediate and low values in Ballenas Channel and on the NGC eddy. In December, the ZB decreased, relative to August, mainly in the NGC and on the mainland side (Fig. 9c). In February (Fig. 9d), the ZB increased relative to December in all the study area, with high and medium values dispersed on the NGC in the eddy area, and high values off the continental coast and in the southern MAR.

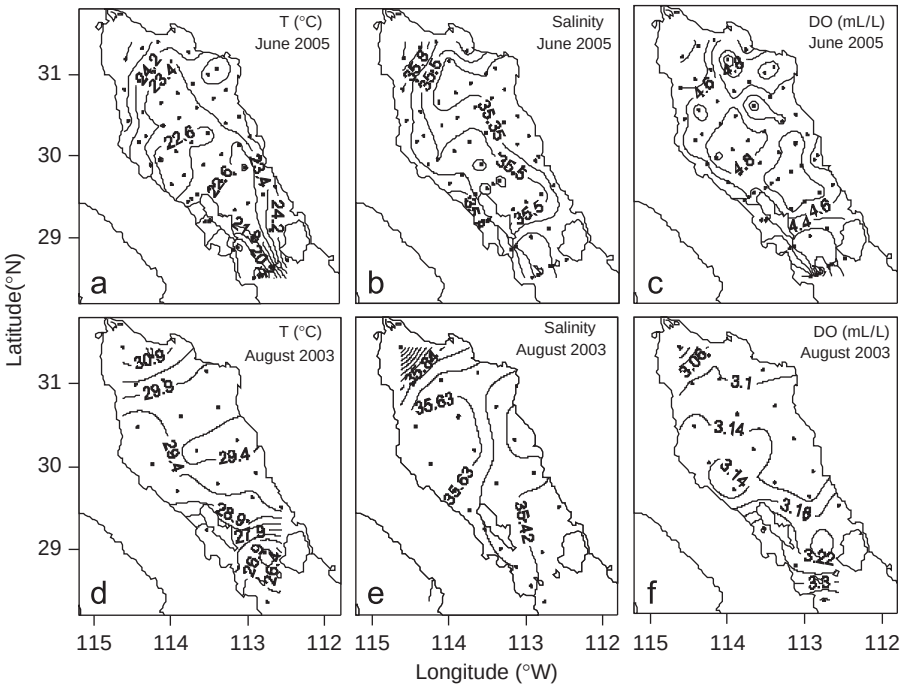

Fig. 5. Surface distribution (top 10 m averages) of temperature (°C), salinity and dissolved oxygen concentration (mL/L) in the northern Gulf of California. (a), (b) and (c) for June 2005; (d), (e) and (f) for August 2003.

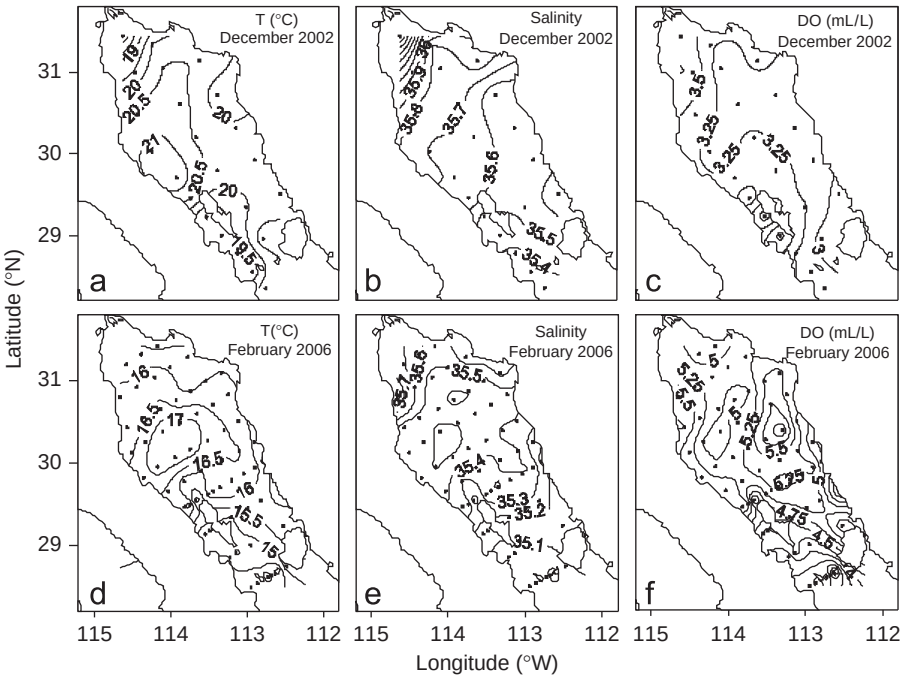

Fig. 6. Surface distribution (top 10 m averages) of temperature (°C), salinity and dissolved oxygen concentration (mL/L) in the northern Gulf of California. (a), (b) and (c) for December 2002; (d), (e) and (f) for February 2006.

3.3.2. *Larval composition*

Fish larvae composition showed a high seasonal variation. The highest number of taxa were found in August (52 taxa included in 28 families) and June (29 taxa included in 20 families), and the lowest in December (19 taxa included in 13 families) and February (10 taxa included in 8 families). The highest number of common species were observed between June and August (14 taxa) and the lowest between August and February (one taxon) (Table 2).

The most abundant species in the cyclonic phase were: *B. panamense* and *Anchoa* spp. larvae in June, and *B. panamense, O. libertate* and *Anchoa* spp. larvae in August. In the anticyclone phase, the most abundant larvae were: *B. panamense* and *E. mordax* in December, and *E. mordax* and *M. productus* in February (Table 2).

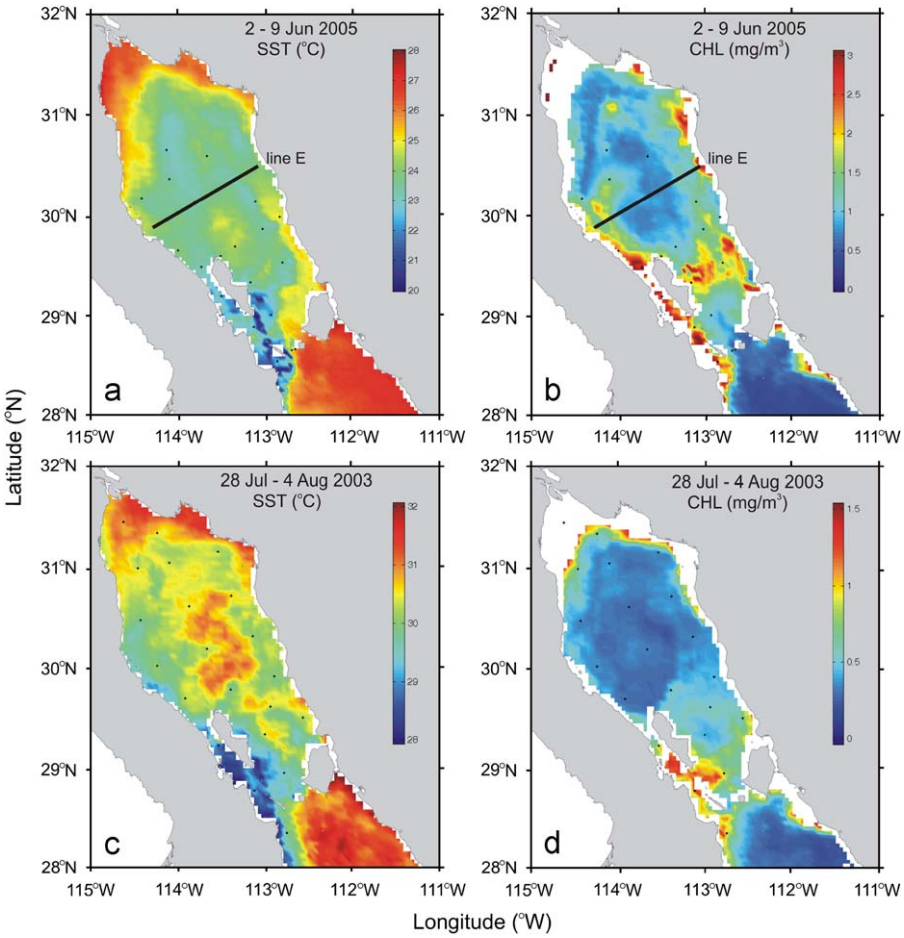

Fig. 7. Satellite images (MODIS) of surface temperature and chlorophyll-*a* concentration in the northern Gulf of California: (a) and (b) June 2005; (c) and (d) August 2003. Dots mark the sampling grids, and Line E is shown. Color scales are not consistent to enhance gradients.

3.3.3. *Larval fish assemblages*

CCA defined station groups (Fig. 10) that varied seasonally in geographic area (Fig. 11), while their LFAs varied in species composition.

Three LFAs were defined in June with high multiple correlations ($r > 0.70$). The salinity was the environmental variable best correlated with axis I ($r = 0.79$) and the ZB with axis II ($r = 0.89$) (Fig. 10a). The LFAs were named according to their geographic area (Fig. 11a, and Table 3): (1) "Current LFA" (7 stations and 24 taxa), located on the mainland side, was in an area with the highest ZB and low bottom depths. This LFA had 516 larvae/10 m^2 and was dominated by *B. panamense, Gobulus crescentalis* and *T. mexicanus* larvae. (2) "Eddy LFA" (10 stations and 29 taxa), located north of the MAR, was in an area with low ZB and the highest values of salinity, temperature and dissolved oxygen. The larval abundance was the lowest (428 larvae/10 m^2), with *G. crescentalis, Anchoa* spp., *Etropus crossotus*, *Lythrypnus dalli, Serranus* spp., *Xenistius californiensis* and *Sphyraena ensis* larvae as the dominant species. (3) The "MAR LFA" (4 stations and 7 taxa) situated around of the MAR had the highest sampling depths and the lowest ZB, salinity, temperature and dissolved oxygen values. This assemblage had the lowest larval abundance (147 larvae/10 m^2) and was dominated by *B. panemense* and *T. mexicanus* larvae.

Four LFAs were defined in August with high multiple correlation in the three ordination axes ($r > 0.79$). The zooplankton sampling depth was the environmental variable best correlated with ordination axis I ($r = 0.89$), and salinity with axis II ($r = 0.86$) (Fig. 10b). The four LFAs (Fig. 11b, and Table 3) were: (1) the "Eddy LFA" (3 sampling stations and 13 taxa), located in the central area of the cyclonic eddy detected by satellite images, was defined by high values of salinity and dissolved oxygen, and low ZB. Its mean larval abundance was of 2848 larvae/10 m^2, and it was dominated by *B. panamense* larvae. (2) The "North LFA" (4 stations and 39 taxa), located north of the Eddy LFA, was defined by the highest temperature and salinity values. This assemblage had the highest larval abundance (4313 larvae/10 m^2) and *O. libertate, E. mordax* and Serranidae larvae were the dominant species. (3) The "Current LFA" (8 stations and 46 taxa) covered the area of the current off the mainland side and was associated to the highest values of ZB. This LFA had a larval abundance of 2756 larvae/10 m^2 dominated by *B. panamense, O. libertate, E. mordax*, *Balistes polylepis, Albula* sp. and *Trichiurus nitens* larvae. (4) The "Ballenas LFA" (4 stations and 23 taxa) located in the Ballenas Channel was defined by the highest sampling depths and dissolved oxygen values, and the lowest ZB and temperature values. This assemblage was characterized by the lowest larval abundance (1260 larvae /10 m^2), and was dominated by *B. panamense* and *Anchoa* spp. larvae.

In December, three LFAs were observed with high multiple correlations ($r > 0.75$). The zooplankton sampling depth was the environmental variable best correlated with axis I ($r = 0.92$) and dissolved oxygen with axis II ($r = 0.78$) (Fig. 10c). The LFAs (Fig. 11c, and Table 3) were: (1) the "Eddy LFA" (5 stations and 11 taxa), located north of the MAR, was determinate by high dissolved oxygen and low ZB values, like in August. This assemblage had a larval abundance of 430 larvae/10 m^2 with dominance of *E. mordax* and *B. panamense* larvae associated with *Citharichthys fragilis* and *E. crossotus* larvae, but with lower

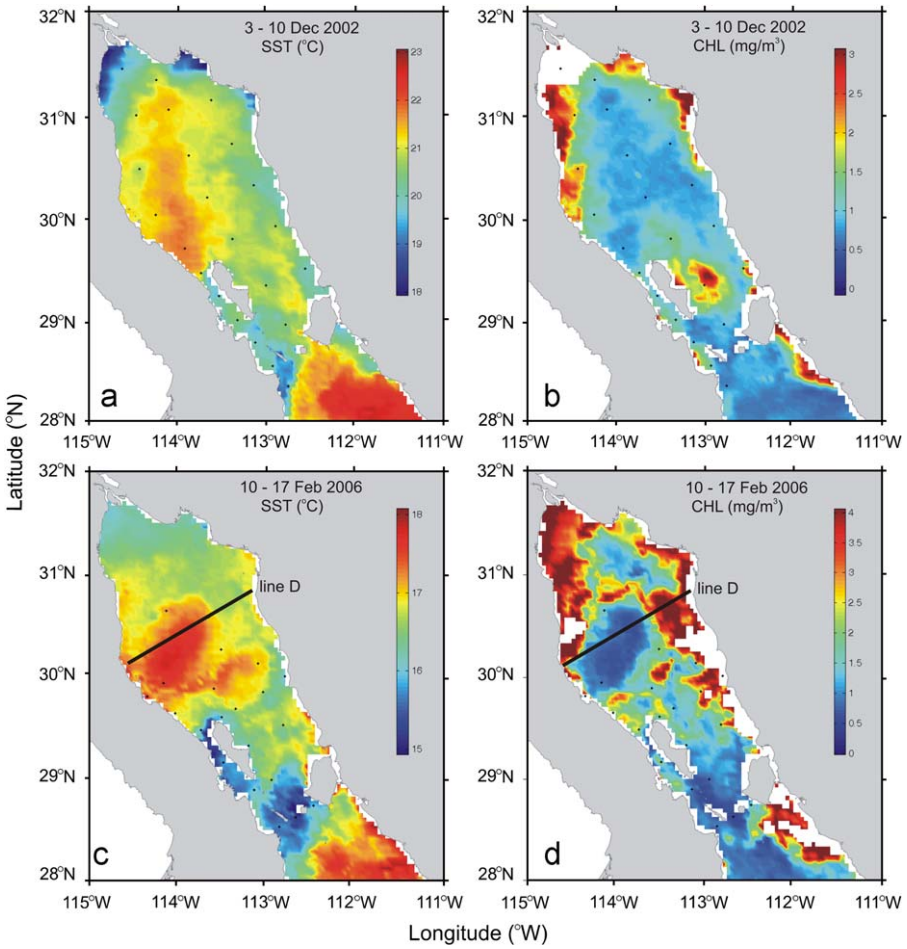

Fig. 8. Satellite images of surface temperature and chlorophyll-*a* concentration in the northern Gulf of California: (a) and (b), for December 2002; (c) and (d), for February 2006. Dots mark the sampling grids and Line D is shown. Color scales are not consistent to enhance gradients.

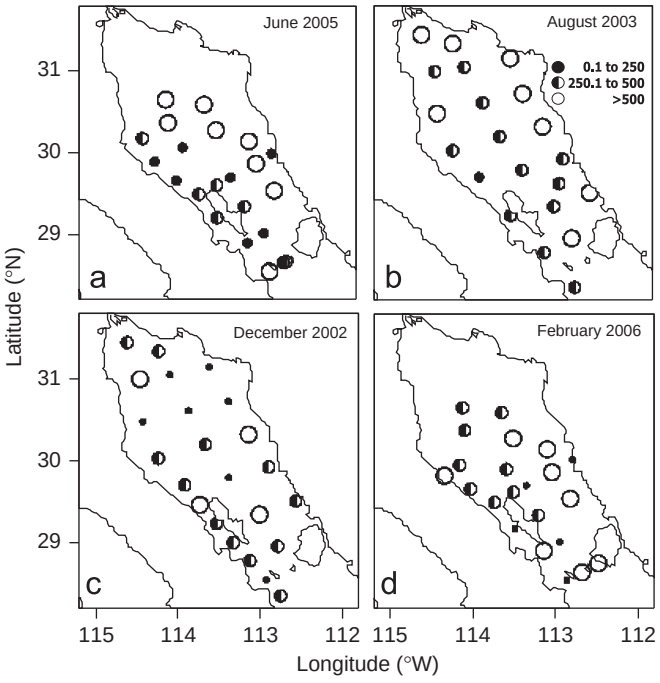

Fig. 9. Spatial distribution of the zooplankton biomass (mL $1000\,m^{-3}$) in the northern Gulf of California. (a) June 2005, (b) August 2003, (c) December 2002 and (d) February 2006.

abundance than the former species. (2) The "North-Current LFA" (9 stations and 14 taxa), situated north of the Eddy LFA and on the coastal current, had the lowest sampling depths, and presented the highest salinities and high ZB values. This assemblage had the lowest larval abundance (275 larvae/$10\,m^2$) and was dominated by *E. mordax* and *B. panamense* larvae associated with *T. mexicanus* and *S. sagax* larvae. (3) The "MAR-Ballenas LFA" (6 stations and 12 taxa) was positioned in Ballenas Channel and the MAR; the area had the highest sampling depths and the lowest salinity and dissolved oxygen values. The highest larval abundance of this cruise was in this LFA (933 larvae/$10\,m^2$), with dominance of *E. mordax* and *B. panamense* larvae associated with *C. fragilis* and *T. mexicanus* larvae.

In February, three larval fish assemblages were also found, with relatively high multiple correlations ($r>0.6$). The temperature was the environmental variable best correlated with axis I ($r=0.96$) and zooplankton biomass with axis II ($r=0.77$) (Fig. 10d). The LFAs (Fig. 11d, and Table 3) were: (1) "Eddy LFA" (5 stations and 8 taxa) was on the well-defined anticyclonic eddy shown by the satellite images. This assemblage was defined by high ZB and the highest values of temperature, salinity and dissolved oxygen. The larvae of *E. mordax* and *M. productus* were dominant, and were associated with *C. fragilis* and *Scomber japonicus* larvae, with a mean larval abundance of 1818 larvae/$10\,m^2$. (2) "Current-Eddy periphery LFA" (10 stations and 10 taxa) were located around the Eddy LFA. This LFA was located in the area with the lowest ZB values and with the highest larval

Table 2
List of species identified during the cruises made in the northern Gulf of California.

Family	Taxa	June		August		December		February	
		$\bar{X}$	%F	$\bar{X}$	%F	$\bar{X}$	%F	$\bar{X}$	%F
Albulidae	*Albula* sp			3.4	46.4				
Anguliforme	Anguilliforme Type 1			0.4	25.0				
	Anguilliforme Type 2			0.1	10.7				
	Anguilliforme Type 3			0.1	10.7				
	Anguilliforme Type 4			0.0	14.3				
Clupeidae	*Etrumeus teres*	1.4	36.4			0.2	12.5		
	Opisthonema libertate	7.3	18.2	12.3	50.0				
	Sardinops sagax					1.4	37.5		
Engraulidae	*Anchoa* spp.	10.1	45.5	9.0	21.4				
	Engraulis mordax			8.0	42.9	45.4	87.5	84.9	100.0
Argentinidae	*Argentina sialis*							0.8	36.4
Bathylagidae	*Leuroglossus stilbius*							1.7	36.4
Phosichthyidae	*Vinciguerria lucetia*	1.8	27.3	0.0	3.6	0.5	8.3		
Synodontidae	*Synodus lucioceps*	0.9	22.7	0.7	32.1	0.4	20.8		
Myctophidae	*Triphoturus mexicanus*	4.8	45.5	0.5	28.6	2.6	41.7		
	Benthosema panamense	32.0	59.1	45.0	64.3	40.6	79.2		
	Diogenichthys laternatus					1.3	12.5		
	Hygophum atratum					0.2	8.3		
Macrouridae	*Caelorinchus scaphopsis*					0.4	12.5	0.1	13.6
Merlucciidae	*Merluccius productus*							6.3	40.9
Ophidiidae	*Lepophidium negropinna*	2.5	18.2						
	Lepophidium stigmatistium	0.4	13.6						
	Lepophidium Type 1			0.1	17.9				
Antennariidae	*Antennarius avalonis*			0.0	14.3				
Melamphaidae	*Melamphaes* sp.			0.0	3.6				
Scorpaenidae	*Sebastes* Type 1							1.2	27.3
	Sebastes Type 2							0.5	27.3
	Pontinus sp.	0.4	13.6	0.1	21.4	0.3	12.5		
	Scorpaena guttata	1.3	18.2						
Triglidae	*Prionotus ruscarius*					0.5	20.8		
Serranidae	Serranidae			3.9	10.7				
	Serranus spp.	3.2	36.4						
	Pronotogrammus multifasciatus	0.7	18.2			0.2	12.5		
Apogonidae	*Apogon retrosella*			0.1	17.9				
Carangidae	*Caranx caballus*			0.0	3.6				
	Caranx sexfasciatus			0.0	14.3				
	Oligoplites saurus inornatus			1.1	35.7				
	Selar crumenophthalmus			0.4	35.7				
	Seriola lalandi	1.1	13.6						
	Carangidae Type 1			0.1	17.9				
Gerreidae	*Diapterus peruvianus*	0.9	13.6						
	Eucinostomus currani			0.1	25.0				
	Eucinostomus gracilis	1.2	22.7	0.2	25.0				
	Eucinostomus dowii	1.3	22.7						
Haemulidae	*Anisotremus davidsonii*			0.4	28.6				
	Xenistius californiensis	2.7	27.3	0.1	28.6				
	Haemulidae Type 1			0.0	10.7				
Sparidae	*Calamus brachysomus*	0.4	13.6						
Scianidae	*Seriphus politus*	0.4	13.6						
	Sciaenidae	0.6	18.2	0.1	14.3				
Mullidae	Mullidae			0.0	17.9				
Pomacentridae	*Chromis punctipinnis*			0.0	3.6				
	Stegastes rectifraenum			0.1	17.9				
Mugilidae	*Mugil cephalus*			0.0	14.3				
Labrisomidae	*Labrisomus xanti*	1.0	18.2						
Bleniidae	*Hypsoblennius gentilis*	0.3	13.6						
Eleotridae	*Eleotris picta*			0.0	10.7	0.3	4.2		
	Eleotridae Type 1			1.1	46.4				
Gobiidae	*Gobulus crescentalis*	7.8	59.1	0.6	14.3				
	Lythrypnus dalli	5.3	50.0	0.6	46.4				
	Gobiidae Type 1			0.9	35.7				
	Gobiidae Type 2			0.0	10.7				
	Gobiidae Type 3			0.2	21.4				
	Gobiidae Type 4			0.0	10.7				
	Gobiidae Type 5			0.6	50.0				
	Gobiidae Type 6			0.0	10.7				
Micodesmidae	MicrodesmidaeType 1			0.3	46.4				
Sphyraenidae	*Sphyraena ensis*	2.7	36.4						
Scombridae	*Auxis* spp.	1.1	22.7	1.1	42.9				
	Scomber japonicus					0.4	16.7	0.6	18.2
	Scomberomorus sierra			0.6	14.3				
Trichiuridae	*Trichiurus nitens*			1.1	28.6				
Paralichthyidae	*Citharichthys* spp.					0.2	8.3		

Table 2 (*continued*)

Family	Taxa	June		August		December		February	
		$\bar{X}$	%F	$\bar{X}$	%F	$\bar{X}$	%F	$\bar{X}$	%F
	Citharichthys fragilis					3.6	45.8	3.6	72.7
	Etropus crossotus	5.8	45.5	0.2	14.3	1.2	37.5		
	Syacium ovale			0.8	46.4				
	Hippoglossina stomata							0.3	18.2
Pleuronectidae	PleuronectidaeType 1					0.5	8.3		
Cynoglossidae	*Symphurus williamsi*	0.4	13.6	1.2	28.6				
	Symphurus Type 1			0.0	14.3				
Balistidae	*Balistes polylepis*			3.8	42.9				

X, mean abundance (larvae/10 m^2); *%F*, frequency of occurrence.

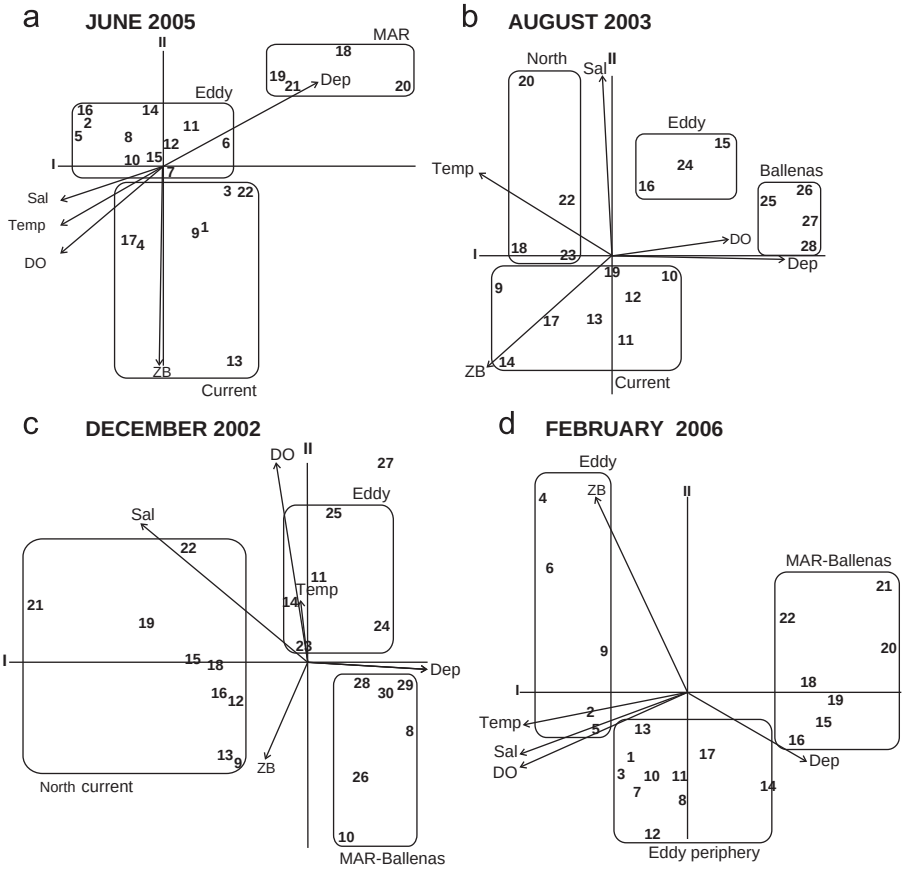

Fig. 10. Graphics of the canonical correspondence analysis (CCA). (a) June 2005, (b) August 2003, (c) December 2002 and (d) February 2006 in the northern Gulf of California.

abundance (1408 larvae/10 m^2). It was dominated by *E. mordax* larvae and by *C. fragilis* and *M. productus* larvae, but the latter two with lower abundance and frequency than the former. (3) The "MAR-Ballenas LFA" (7 stations and 9 taxa) had the highest sampling depths, low ZB values and the lowest temperature, salinity and dissolved oxygen. Its larval abundance was the lowest of the cruise (1102 larvae/10 m^2) and was dominated by *E. mordax* larvae associated with *Leuroglossus stilbius and Sebastes* sp.

4. Discussion

4.1. Seasonal and interannual variability

Seasonal changes of LFAs and their boundaries in the NGC were analyzed in relation with the seasonal changes of the main oceanographic structures detected by satellite and *in situ* data, with the additional aid of a numerical model. For this purpose, data from four cruises made in different years were used: June 2005 and August 2003 representing the cyclonic phase, and December 2002 and February 2006 representing the anticyclonic phase of the seasonal circulation. Oceanographic conditions at the times of our cruises were representative of the respective phases of the seasonal cycle (Lavín and Marinone, 2003). From the biological point of view, there are studies (Moser et al., 1974; Aceves-Medina et al., 2004) which, although not individually oriented to the seasonal scale, suggested that there are seasonal changes in fish larvae, and our data agree with and further those early findings. In addition, studies focusing on the interannual time scale have concluded that the physical and biological seasonal variations in the GC are larger than the interannual variations, including El Niño and La Niña events (e.g., Green-Ruíz

and Hinojosa-Corona, 1997; Santamaría-del-Angel et al., 1994b; Sánchez-Velasco et al., 2000; Hidalgo-González and Alvarez-Borrego, 2004). Therefore our data set, although collected in different years, provided a good representation of the contrasting conditions during the two seasonal circulation phases of the NGC.

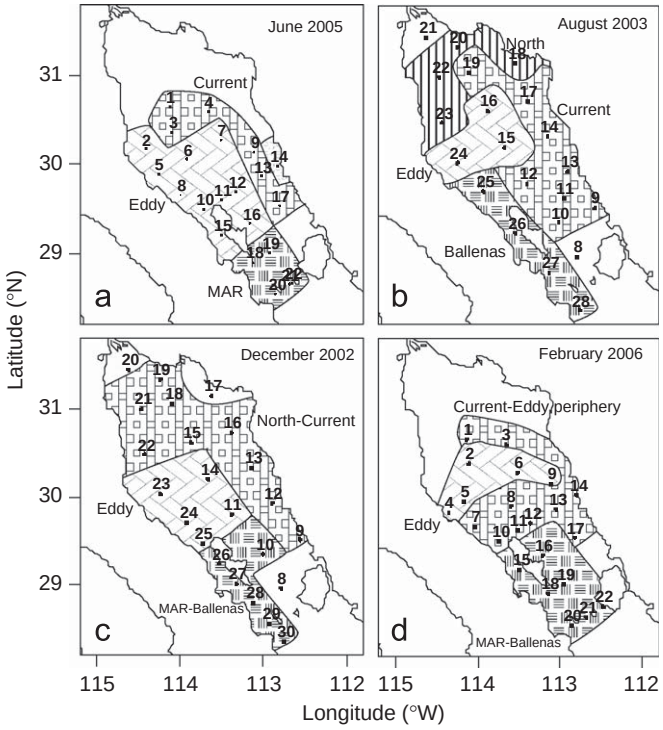

Fig. 11. Location of larval fish assemblages for the four cruises made in the northern Gulf of California. (a) June 2005, (b) August 2003, (c) December 2002 and (d) February 2006.

4.2. Larval fish assemblages and their boundaries

The location of the areas occupied by the LFAs (Fig. 11) was related with specific hydrodynamic features of the NGC and their seasonal evolution: (i) the coastal current on the mainland shelf, (ii) the central eddy and (iii) the MAR and Ballenas Channel. In addition, the dominant species also exhibited seasonal changes, which suggested a coupling between the environment and the spawning species. An interesting feature is the seasonal dominance of species like *M. productus*, *O. libertate* and *E. mordax*, that have been identified as part of the fish guild characteristic of eastern boundary current systems (e.g., Fiedler, 1986; Olivar and Shelton, 1993; Landaeta et al., 2008).

In this Section we discuss the biophysical characteristics of the three areas, and in Section 4.3 an integral seasonal model is proposed that includes the variation of those species.

(i) The Current LFAs

The LFAs found on the mainland shelf contained the highest concentrations of ZB and larval fish abundance during both the cyclonic and the anticyclonic phases. This may be related with the findings of Santamaría-del-Angel et al. (1994a) that the oriental coast of the NGC had high chlorophyll concentration throughout the year. There are several possible explanations for the biological richness of the LFA Current area. Among the local enriching hydrodynamic processes over the mainland shelf we can identify mixing by tidal currents, by vertical convection and by the breaking of internal waves. Convection would be most energetic in winter (Reyes and Lavín, 1997), while internal waves would be most important in summer. Since the wind in the GC is northwesterly most of the year, except in summer (Bordoni et al., 2004), coastal upwelling enriches the Current LFA area in the anticyclonic phase (Santamaría-del-Angel et al., 1994a; Lluch-Cota, 2000). In addition, in the cyclonic phase the coastal current may bring into the Current LFA area

Table 3
Dominant species of the sampling stations groups and their larval fish assemblages in the northern Gulf of California determined by the Olmstead–Tukey test.

	June 2005						August 2003								December 2002						February 2006					
	Eddy		Current		MAR-Ballenas		Eddy		North		Current		Ballenas		Eddy		North-Current		MAR-Ballenas		Eddy		Current eddy periphery		MAR-Ballenas	
Dominant Taxon	*X*	*%F*	*X*	*%F*	*X*	*%F*	*X*	*%F*	*X*	*%F*	*X*	*%F*	*X*	*%F*	*X*	*%F*	*X*	*%F*	*X*	*%F*	*X*	*%F*	*X*	*%F*	*X*	*%F*
Albula sp.											224	87														
Anchoa spp.	81	60											457	75												
Balistes polylepis											222	100														
Benthosema panamense			333	86	85	75																				
Benthosema panamense							2784	100			1593	100	652	100	138	80	36	89	541	100						
Engraulis mordax									890	100	90	75			243	100	190	100	293	100	1279	100	1327	100	935	100
Etropus crossotus	47	60																								
Gobulus crescentalis	51	89	29	71																						
Lythrypnus dalli	33	60																								
Merluccius poductus																					345	80				
Opisthonema libertate									1307	100	168	100														
Serranidae									523	75																
Serranus spp.	24	60																								
Sphyraena ensis	17	40																								
Trichiurus nitens											68	75														
Triphoturus mexicanus			25	43	45	100																				
Xenistius californiensis	21	40																								
Number of taxa	29		24		7		13		39		46		23		11		14		12		8		10		9	
Number of stations	10		7		4		3		4		8		4		5		9		6		5		10		7	
Mean larval abundance (larvae/10 m^2)	428		516		147		2848		4313		2756		1260		430		275		933		1818		1408		1102	

X, mean abundance; *%F*, frequency of ocurrence.

properties such as nutrients and primary production biomass from the MAR and Ballenas Channel that are enriched by tidal mixing and convergence-induced upwelling, while in the anticyclonic phase it could do the same from the tidal-mixing-enriched Upper Gulf (Hernández-Ayón et al., 1993). These mechanisms probably turn the mainland shelf into an important enrichment area for the pelagic ecosystem in the NGC.

(ii) The Eddy LFAs

The LFAs associated with the seasonally reversing eddy in the center of the NGC showed better definition in the mature circulation phases. (a) In February, during the anticyclonic circulation phase, the eddy was warmer and had lower chlorophyll-*a* concentration than its periphery, while ZB and larval abundance were intermediate, but specific richness was low. The epipelagic *E. mordax* and the deep demersal *M. productus* contributed with >90% of the total larval abundance observed in the eddy. The latter species was found only in this LFA, indicating that its spawning was associated with eddy conditions. (b) During August, when the mature cyclonic eddy was cooler and with lower surface chlorophyll-*a* concentration than the surrounding area, low ZB and intermediate larval abundance were recorded. Although the number of species that spawned in this period increased notably, the mesopelagic *B. panamense* was the only dominant species, albeit with lower abundance than in the surrounding areas (such as in the Current LFA area).

Thus we found ZB to be lower in the cyclonic than in the anticyclonic eddy, and both ZB and larval abundance to be lower than in the surrounding areas (the mainland shelf, the MAR, the Upper Gulf) in both circulation phases. In general nutrients and productivity in the NGC are higher in winter than in summer (Alvarez-Borrego et al., 1978; Hidalgo-González and Alvarez-Borrego, 2004). The low biological enrichment in the central eddy area may be because the eddy is formed by the overall circulation of the Gulf rather than by Ekman pumping, and because of winter vertical convection. There would be no continuous upwelling of nutrients into the surface layer during the cyclonic phase (summer), while in winter (anticyclonic phase) a deep surface mixed layer would not be propitious for high primary productivity. However, in general the effects of eddies on ZB and LFAs is not limited to a simple scheme of enrichment or not from upwelling/downwelling; the effects can be influenced by the eddy physical structure and processes of entrainment of water masses at the formation stage (Griffiths and Wadley, 1986; Muhling et al., 2007).

(iii) The MAR and Ballenas Channel LFAs

Contrary to the Current LFA, the LFAs located in the MAR and Ballenas Channel presented low ZB and low larval fish abundance (except in December probably because the larger number of stations covered a wider area). The area of this LFA had marked seasonal changes joining the MAR and Ballenas Channel in the anticyclonic period (December and February), while separating the MAR in June and Ballenas Channel in August; this was probably an indicator of the oceanographic complexity of the zone. There are several studies describing the mechanisms that may induce a continuous nutrient enrichment of this area (Alvarez-Borrego et al., 1978; Paden et al., 1991; Argote et al., 1995; López et al., 2006). These studies show that the most persistent upwelling occurs in Ballenas Channel, where tidal mixing and convergence-induced upwelling generate the lowest SST of the Gulf during the year. This minimum SST is limited to the south and north by sharp SST and chlorophyll fronts, which frequently show convolutions, eddies and filaments, resulting in a zone with high turbulence and instability, but highly fertile. Studies on larval fish assemblages and their relation with SST identified this habitat as a well-defined assemblage, but with low number of species and low fish larvae abundance (e.g., Avalos-García et al., 2003; Sánchez-Velasco et al., 2004). Our study concurs with those observations, and we propose that during the cyclonic phase of the circulation (June–September) the enriched waters from this source are exported to the shelf area off the mainland where they affect positively the Current LFA.

4.3. A conceptual model

The relationships between the seasonal changes in LFAs and the oceanographic dynamics of the NGC are summarized below by a conceptual model, which is based on our observations and on previous work (e.g., Moser et al., 1974; Alvarez-Borrego et al., 1978; Santamaría-del-Angel et al., 1994a; Lavín and Marinone, 2003; Aceves-Medina et al., 2004; Peguero-Icaza et al., 2008). Explanations of some of the biophysical features are offered, but they should be considered as propositional, because of the scarcity of data, especially of chlorophyll and nutrients (Hidalgo-González and Alvarez-Borrego, 2004).

In the early cyclonic phase (June), the coastal current on the mainland shelf was present, but the central eddy may have been in the process of formation. Temperature and stratification (thermocline strength) were also in the increase at this time, resulting in an environment favorable for phytoplankton blooms. As explained above, several enriching mechanisms could explain why the maximum values of ZB, fish larvae abundance and specific richness were recorded on the Current LFA area, where coastal demersal species (e.g., *G. crescentalis, L. dalli*) co-dominated with mesopelagic species (*B. panamense*). In the Eddy LFA area, coastal demersal species dominated, but with lower abundance than in the Current LFA area. The cool conditions created by mixing in the MAR LFA area caused the lowest abundance of this season, and this LFA to be dominated by mesopelagic species.

When the cyclonic phase matured (August), the physical and nutrient conditions described for June continued, except that stratification was stronger and the cyclonic eddy was firmly established. Consequently, the ZB and species richness were again higher in the Current LFA area than in the Eddy LFA area. The composition of the LFAs, however, presented a dramatic change relative to June, probably because of the stronger stratification: eastern boundary current species (*O. libertate and E. mordax*) and mesopelagic species (*B. panamense*) took the dominance from the coastal demersal species. *O. libertate*, *E. mordax* and *B. panamense* co-dominated in the Current LFA area. *B. panamense* dominated in the Eddy LFA area, but its abundance was lower than in the Current LFA area. Again, in the mature cyclonic period the MAR and Ballenas Channel had the lowest larval abundance of the region and intermediate ZB values.

The early anticyclone phase (December) was characterized by a rapidly changing environment. The circulation of the NGC had begun to reverse, the SST decreased steadily, and the strong NW winds generated upwelling on the mainland side. Vertical mixing by the wind and cooling-induced convection created a surface mixed layer that reached at least ~50 m depth. The ZB and the species richness decreased in all the NGC, but these variables continued to be higher in the Current LFA area than in the Eddy LFA area; this was probably due to higher nutrient availability in the mainland shelf (due to local processes and to advection from the Upper Gulf) than in the eddy (entrainment by surface mixed

layer deepening). In these conditions, *O. libertate* larvae were absent, while *E. mordax* (eastern boundary species) and *B. panamense* (mesopelagic) continued dominating in all the NGC, with higher abundance in the MAR and Current LFA areas than in the Eddy LFA area. The biological indicators showed a tendency to spatial homogenization in this phase, in contrast with the cyclonic phase, probably reflecting better trapping capacity in the latter.

In the mature anticyclonic phase (February), the central eddy and the southward coastal current on the mainland shelf were well established. The sources of nutrients for the mainland shelf (upwelling, mixing, and advection from the Upper Gulf) continued to operate, while that for the eddy (vertical entrainment) had probably become unimportant as the mixed layer reached its maximum depth (~100 m). Consequently, the eddy showed lower chlorophyll concentration, ZB and species richness than the mainland shelf area. These conditions were associated with the enhancement in abundance of eastern boundary current species and with a drastic decrement in species richness in all the NGC. *E. mordax* larvae dominated in the Current and the Eddy LFA areas, but with the highest abundance in the Current LFA area. Dominant in the Eddy LFA were *M. productus* larvae, an eastern boundary current species.

These conditions continued until temperature and stratification started increasing in the spring, leading to the conditions described above for June, with coastal demersal and mesopelagic fish larvae dominating the LFAs of the NGC.

5. Conclusions

This observational study found that throughout the seasonal cycle the definition of LFAs in the northern Gulf of California was related with specific oceanographic features: the seasonally reversing central eddy and coastal current on the mainland continental shelf, and the hydrographic conditions of the MAR and Ballenas Channel. We propose that the dramatic seasonal changes of the hydrography and circulation trigger the spawning of species that are favored by the environmental conditions of each area, which implies a close and predictable coupling between the environmental evolution and the spawning species. In the early cyclonic phase (June), coastal demersal species (e.g., *Gobulus crescentalis, Lythrypnus dalli*) dominated together with mesopelagic species (*Benthosema panamense*), with the highest abundance on the mainland shelf coastal current area. In the mature cyclonic phase (August), species characteristic of eastern boundary current system such as *Opisthonema libertate* and *Engraulis mordax* displaced the demersal species and became dominant together with mesopelagic species (*B. panamense*) in the Current LFA area; the mesopelagic species dominated in the Eddy LFA area. In the early anticyclonic phase (December), *O. libertate* larvae were absent and *E. mordax* and *B. panamense* continued dominating in all the NGC, with higher abundance in the MAR than in the Current LFA and Eddy LFA areas. In the mature anticyclonic phase (February), *E. mordax* larvae dominated in the Current and the Eddy LFA areas, but with the highest abundance in the former, while *M. productus* larvae (an eastern boundary current species) appeared as dominant in the Eddy LFA area.

The Current LFA area stands out as the richest throughout the seasonal cycle (it presented the highest values of chlorophyll and zooplankton biomass and high larval abundance), which suggests that this area has an important role in the pelagic ecosystem functionality of the NGC. The seasonal dominance of species like *M. productus*, *O. libertate, E. mordax,* members of the fish guild characteristic of eastern boundary current systems, implies that (although in smaller scale) the NGC has high-productivity conditions similar to those of the most productive oceanic ecosystems of the world.

Acknowledgments

This work was supported by SEP-CONACyT (Contracts 2004-C01-46349, D41881-F and 44055), CGPI-Instituto Politécnico Nacional (project codes 20080486 and 20090578), and Secretaría de Marina of Mexico (project *Circulación del Golfo de California mitad norte*). We acknowledge the efforts of Tte. Corb. SMAM. L. Ocean. Francisco Padilla Ozuna (Secretaría de Marina) in organizing the June 2005 and February 2006 cruises. Thanks to Alberto Amador (CICESE) and Alma Rosa Padilla (Instituto de Ciencias del Mar y Limnologia, Universidad Nacional Autónoma de México) for physical data collection and processing, and to Carlos Cabrera (CICESE) for satellite data handling. Thanks to two anonymous referees, whose comments greatly improved this article.

References

Aceves-Medina, G., Jiménez-Rosenberg, S.P.A., Hinojosa-Medina, A., Funes-Rodríguez, R., Saldierna-Martínez, R.J., Smith, P.E., 2004. Larval fish assemblages in the Gulf of California. Journal of Fish Biology 65, 832–847.

Alvarez-Borrego, S., Rivera, J.A., Gaxiola-Castro, G., Acosta-Ruiz, M.J., Schwatzlose, A., 1978. Nutrientes en el Golfo de California. Ciencias Marinas 5, 53–71.

Alvarez-Borrego, S., Lara-Lara, R., 1991. The physical environment and primary productivity of the Gulf of California. In: Simoneit, B.R.T., Dauplin, J.P., (Eds.), Gulf and peninsular province of the California, Monografía, Mem. Amer. Assoc. Petrol. Geol., pp. 555–567.

Argote, M.L., Amador, A., Lavín, M.F., Hunter, J.R., 1995. Tidal dissipation and stratification in the Gulf of California. Journal of Geophysical Research 100, 16103–16118.

Avalos-García, C., Sánchez-Velasco, L., Shirasago, B., 2003. Larval fish assemblages in the Gulf of California and their relation to hydrographic variability (Autumn 1997–Summer 1998). Bulletin of Marine Science 72 (1), 63–76.

Bakun, A., 1996. Fronts and eddies as key structures in the habitat of marine fish larvae: opportunity, adaptive response and competitive advantage. Scientia Marina 70, 105–122.

Beier, E., 1997. A numerical investigation of the annual variability in the Gulf of California. Journal of Physical Oceanography 27, 615–632.

Bordoni, S., Ciesielski, P.E., Johnson, R.H., McNoldy, B.D., Stevens, B., 2004. The low-level circulation of the North American Monsoon as revealed by QuikSCAT. Geophysical Research Letters 31, L10109.

Carrillo, L., Lavín, M.F., Palacios-Hernández, E., 2002. Seasonal evolution of the geostrophic circulation in the northern Gulf of California. Estuarine, Coastal and Shelf Science 54 (2), 157–173.

Cudney-Bueno, R., Lavín, M.F., Marinone, G., Raimondi, P.T., Shaw, W.W., 2009. Rapid effects of marine reserves via larval dispersal. PLoS ONE 4 (1), e4140.

De La Cruz-Agüero, G., 1994. ANACOM: Sistema para el análisis de comunidades. Ver 3.0. Manual del Usuario. CICIMAR-IPN, La Paz, Baja California Sur, México, 99 p.

Field, J.G., Clarke, K.R., Warwick, R.M., 1982. A practical strategy for analyzing multispecies distribution patterns. Marine Ecology Progress Series 8, 37–52.

Fiedler, P.C., 1986. Offshore entrainment of anchovy spawning habitat, eggs, and larvae by a displaced eddy in 1985. California Cooperative Oceanic Fisheries Investigation Reports 26, 144–152.

Green-Ruíz, Y., Hinojosa-Corona, A., 1997. Study of the spawning area of the northern anchovy in the Gulf of California from 1990 to 1994, using satellite images of sea surface temperature. Journal of Plankton Research 19, 957–968.

Griffiths, F.B., Wadley, V., 1986. A synoptic comparison of fishes and crustaceans from a warm-core eddy, the east Australian Current, the coral sea and the Tasman Sea. Deep Sea Research 33, 1907–1922.

Hammann, M.G., Nevarez-Martínez, M.O., Green-Ruíz, Y., 1998. Spawning habitat of the Pacific sardine (*Sardinops sagax*) in the Gulf of California: eggs and larval distribution 1956–1957 and 1971–1991. California Cooperative Oceanic Fisheries Investigation Reports 39, 169–179.

Hernández-Ayón, J.M., Galindo-Bect, M.S., Flores-Báez, B.P., Alvarez-Borrego, S., 1993. Nutrient concentrations are high in the turbid waters of the Colorado River Delta. Estuarine, Coastal and Shelf Science 37, 593–602.

Hidalgo-González, R.M., Alvarez-Borrego, S., 2004. Total and new production in the Gulf of California estimated from ocean color data from the satellite sensor SeaWIFS. Deep-Sea Research II 51, 739–752.

Iles, T.D., Sinclair, M., 1982. Atlantic herring: stock discreetness and abundance. Science 215, 627–633.

Kramer, D., Kalin, M.J., Stevens, E.G., Thrailkill, J.R., Zweifel, J.R., 1972. Collecting and processing data on fish eggs and larvae in the California Current region. NOAA Technical Report NMFSC.

Landaeta, M.L., Rodrigo, V., Letelier, J., Castro, L.R., 2008. Larval fish assemblages off central Chile upwelling ecosystem. Revista de Biología Marina y Oceanografía 43 (3), 571–586.

Lavín, M.F., Marinone, S.G., 2003. An overview of the physical oceanography of the Gulf of California. In: Velasco, O., Sheimbaum, J., Ochoa, J.J. (Eds.), Nonlinear Processes in Geophysical Fluid Dynamics. Kluwer Academia Publishers, Dordrecht, The Netherlands, pp. 173–204.

Lavín, M.F., Castro, R., Beier, E., Amador, A., 2009. SST, thermohaline structure and circulation in the southern Gulf of California in June 2004, during the North American Monsoon Experiment. Journal of Geophysical Research 114, C02025, doi:10.1029/2008JC004896.

López, M., Candela, J., Argote, M.L., 2006. Why does the Ballenas Channel have the coldest SST in the Gulf of California? Geophysical Research Letters 33, L11603.

Lopez-Calderon, J., Martinez, A., Gonzalez-Silvera, A., Santamaría-del-Angel, E., Millan-Nuñez, E., 2008. Mesoscale eddies and wind variability in the northern Gulf of California. Journal of Geophysical Research 113, C10001, doi:10.1029/2007JC004630.

Lluch-Cota, S-E., 2000. Coastal upwelling in the eastern Gulf of California. Oceanologica Acta 23, 731–740.

Marinone, S.G., 2003. A three dimensional model of the mean and seasonal circulation of the Gulf of California. Journal of Geophysical Research 108 (C10), 3325.

Marinone, S.G., Ulloa, M.J., Parés-Sierra, A., Lavín, M.F., Cudney-Bueno, R., 2008. Connectivity in the northern Gulf of California from particle tracking in a three-dimensional numerical model. Journal of Marine Systems 71, 149–158.

Moser, H.G., Ahlstrom, E.H., Kramer, D., Stevens, E.G., 1974. Distribution and abundance of fish eggs and larvae in the Gulf of California. California Cooperative Oceanic Fisheries Investigation Reports 17, 112–128.

Moser, H.G., Smith, P., 1993. Larval fish assemblages and oceanic boundaries. Bulletin of Marine Science 53 (2), 28–289.

Moser, G.H., 1996. The early stages of fishes in the California Current region, California Cooperative Oceanic Fisheries Investigation Atlas no.33, NOAA-NMFS-SFSC, Allen press, Inc., Lawrence, Kansas.

Muhling, B.A., Beckley, L.E., Olivar, M.P., 2007. Ichthyoplankton assemblage structure in two meso-scale Leeuwin Current eddies, eastern Indian Ocean. Deep Sea Research II 54, 113–1128.

Navarro-Olache, L.F., Lavín, M.F., Alvarez-Sánchez, L.G., Zirino, A., 2004. Internal structures of SST features in the central Gulf of California. Deep Sea Research II 51, 673–687.

Olivar, M.P., Shelton, P.A., 1993. Larval fish assemblages of the Benguela Current. Bulletin of Marine Science 52 (2), 450–474.

Paden, C.A., Abbott, M.R., Winant, C.D., 1991. Tidal and atmospheric forcing of the upper ocean in the Gulf of California. Part I: sea surface temperature variability. Journal of Geophysical Research 96 (C10), 18337–18359.

Palacios-Hernández, E., Beier, E., Lavín, M.F., Ripa, P., 2002. The effect of winter mixing on the circulation of the northern Gulf of California. Journal of Physical Oceanography 32, 705–728.

Pegau, W.S., Boss, E., Martínez, A., 2002. Ocean color observations of eddies during the summer in the Gulf of California. Geophysical Research letters 29 (9), 1–3.

Peguero-Icaza, M., Sánchez-Velasco, L., Lavín, M., Marinone, G., 2008. Larval fish assemblages, hydrographic and circulation in the Gulf of California. Estuarine Coastal and Shelf Science 30, 1–12 〈http://dx.doi.org/10.1016/j.ecss.2008.04.008〉.

Reyes, A.C., Lavín, M.F., 1997. Effects of the autumn–winter meteorology upon the surface heat loss in the northern Gulf of California. Atmosfera 10, 101–123.

Ripa, P., 1997. Toward a physical explanation of the seasonal dynamics and thermodynamics of the Gulf of California. Journal of Physical Oceanography 27, 597–614.

Sánchez-Velasco, L., Shirasago, B., Cisneros-Mata, M., Avalos-García, C., 2000. Spatial distribution of small pelagic fish larvae in the Gulf of California and its relation to the El Niño1997–1998. Journal of Plankton Research 28, 1611–1618.

Sánchez-Velasco, L., Avalos-García, C., Renteria-Cano, M., Shirasago, B., 2004. Fish larvae abundance and distribution in the central Gulf of California during strong environmental changes (1997–1998 El Niño and 1998–1999 La Niña). Deep Sea Research 11 (51), 711–722.

Sánchez-Velasco, L., Beier, E., Avalos-García, C., Lavín, M., 2006. Larval fish assemblages and geostrophic circulation in Bahía de La Paz and the surrounding southwestern region of the Gulf of California. Journal of Plankton Research 28, 1–18.

Santamaría-del-Angel, E., Alvares-Borrego, S., Müller-Karger, F.E., 1994a. Gulf of California biogeographic regions based on coastal zone color scanner imagery. Journal of Geophysical Research 99 (C4), 7411–7421.

Santamaría-del-Angel, E., Alvares-Borrego, S., Müller-Karger, F.E., 1994b. The 1982–1984 El Niño in the Gulf of California as seen in coastal zone color scanner imagery. Journal of Geophysical Research 99 (C4), 7423–7431.

Smith, P.E., Richardson, S.L., 1979. Técnicas modelo para prospección de huevos y larvas de peces pelágicos. FAO. Documentos Técnicos de Pesca.

Sokal, R.R., Rohlf, J., 1985. Biometry. Blume, Barcelona, Spain.

Ter Braak, C.J.F., 1986. Canonical correspondence analysis: a new eigenvector technique for multivariate direct gradient analysis. Ecology 67 (5), 60–71.

Zamudio, L., Hogan, P., Metzger, J.E., 2008. Summer generation of the southern Gulf of California eddy train. Journal of Geophysical Research 113, 1–21, C06020.